What is being measured with P-bearing NMR probe molecules adsorbed on zeolites?

Carlos Bornes,[a] Michael Fischer,[b] Jeffrey A. Amelse,[a] Carlos F. G. C. Geraldes,[c] João Rocha[a] and Luís Mafra*[,a]

[a] CICECO, Aveiro Institute of Materials, Department of Chemistry, University of Aveiro, 3810-193 Aveiro, Portugal.

[b] Faculty of Geosciences, University of Bremen, 28359 Bremen, Germany; MAPEX Center for Materials and Processes, University of Bremen, 28359 Bremen, Germany.

[c] Department of Life Sciences and Coimbra Chemistry Center, Faculty of Science and Technology, University of Coimbra, 3000-393 Coimbra, Portugal; CIBIT-Coimbra Institute for Biomedical Imaging and Translational Research, Edifício do ICNAS, 3000-548 Coimbra, Portugal.

KEYWORDS Zeolite acidity, Probe molecules, TMPO, solid-state NMR, AIMD, ^{31}P NMR, confinement effect

ABSTRACT: Elucidating the nature, strength and siting of acid sites in zeolites is fundamental to fathom their reactivity and catalytic behavior. Despite decades of research, this endeavor remains a major challenge. Trimethylphosphine oxide (TMPO) has been proposed as a reliable probe molecule to study the acid properties of solid acid catalysts, allowing the identification of distinct Brønsted and Lewis acid sites and the assessment of Brønsted acid strengths. Recently, doubts have been raised regarding the assignment of the ^{31}P NMR resonances of TMPO-loaded zeolites. Here, it is shown that a judicious control of TMPO loading combined with two-dimensional ^{1}H-^{31}P HETCOR solid-state NMR, DFT and ab initio molecular dynamics (AIMD)-based computational modelling provide an unprecedented atomistic description of the host-guest and guest-guest interactions of TMPO molecules confined within HZSM-5 molecular-sized voids. ^{31}P NMR resonances usually assigned to TMPO molecules interacting with Brønsted sites of different acid strength arise instead from both changes in the probe molecule confinement effects at ZSM-5 channel system and the formation of protonated TMPO dimers. Moreover, DFT/AIMD show that the ^{1}H and ^{31}P NMR chemical shifts strongly depend on the siting of the framework aluminum atoms. This work overhauls the current interpretation of NMR spectra, raising important concerns about the widely accepted use of probe molecules for studying acid sites in zeolites.

INTRODUCTION

Zeolites are crystalline nanoporous materials with three-dimensional frameworks built up of silicon, oxygen and aluminum atoms, *i.e.*, aluminosilicates. The diversity of zeolite topologies combined with high pore volume and adsorption capacity, shape selectivity and thermal stability enable their use in the refining and petrochemical industries as solid acid catalysts. Unfortunately, providing an accurate and complete characterization of the acid properties of zeolites, namely acid site density, nature, strength, and accessibility, remains a major challenge. Spectroscopists have addressed this issue using several probe molecules that interact specifically with Brønsted and Lewis acid sites.[1] Certain protocols mix diverse probe molecules that selectively populate the different inner zeolite cavities and elucidate the nature of the acid sites.[2,3]

^{31}P NMR chemical shifts of phosphines have been widely used to study the acid properties of solid catalysts.[4,5] Trimethylphosphine oxide (TMPO) has been the most widely used probe molecule in solid-state NMR studies of zeolites,[6–8] metal-organic frameworks,[9,10] heteropoly acids,[11,12] etc.,[4] due to its high sensitivity, chemical stability, and because it is safer than the also used trimethylphosphine.[13] The small kinetic diameter of TMPO, *ca.* 5.5 Å, allows its diffusion in most medium-pore size materials, in contrast with the larger tributylphosphine oxide and triphenylphosphine oxide molecules, commonly used to study the external surface of such materials.[13] Moreover, TMPO interacts with Brønsted and Lewis acid sites, giving ^{31}P NMR chemical shifts ranging from *ca.* 53 to 86 ppm and *ca.* 55 to 60 ppm, respectively.[13,14] However, the interpretation of ^{31}P NMR spectra of TMPO-loaded zeolites remains controversial. While some authors contend that TMPO interaction with Brønsted and Lewis acid sites gives rise to ^{31}P NMR resonances in distinct spectral regions,[14,15] others argue that they overlap.[16,17] Furthermore, recent studies show that two TMPO molecules may gather at the same acid site, forming $(TMPO)_2H^+$ dimers.[18,19] The diversity of TMPO binding modes further hinders our understanding of the nature of the TMPO-acid interaction in microporous materials, requiring the tandem use of spectroscopic and computational tools.

A linear correlation between ^{31}P NMR chemical shifts and Brønsted acid strength has been derived from computational modeling of TMPO molecules interacting with zeolite clusters.[20] This correlation has been used to both identify the distribution of Brønsted acid site strength in zeolites[15]

and to classify solid acid catalysts according to their acid strength.[9] However, calculated deprotonation energies, considered a true measure of Brønsted acid site strength,[21,22] provide strong evidence for the homogeneity of acid strength in high Si/Al ratio zeolites, *i.e.*, the zeolite Brønsted acid strength is independent of the acid site location[23,24] and zeolite framework type.[21,22] An intriguing question is what is actually being measured by means of probe molecules adsorbed on acid zeolites.[25,26] In contrast with deprotonation energy calculations that afford the intrinsic acid strength, probe molecule measurements result from an ensemble of properties, such as the zeolite acid site strength and probe molecule base strength, and also witness the stabilization of the interacting probe molecule by the surrounding framework (confinement effects). Hence, the study of zeolite acidity assisted by probe molecules requires an in-depth description of the host-guest and guest-guest interactions, which is not available in most studies. Recent developments in *ab initio* molecular dynamics (AIMD) provide new insights on the reaction mechanisms of organic molecules confined in acid zeolites.[27,28] To the best of our knowledge, the capabilities of these methods have hardly been exploited to study the interaction of probe molecules with acid centers in zeolites.[29,30]

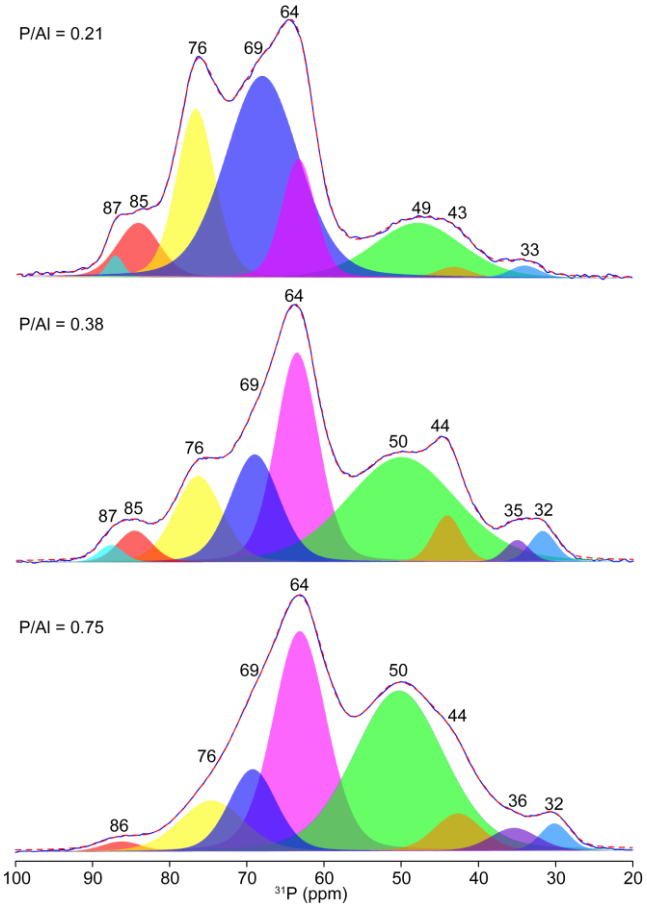

Figure 1. ^{1}H-decoupled ^{31}P MAS NMR spectra of HZSM-5 samples loaded with 1 (P/Al = 0.21), 2 (P/Al = 0.38) and 4 mg (P/Al = 0.75) of TMPO.

Herein, we provide unprecedented insight into the status of TMPO molecules adsorbed in HZSM-5, challenge certain widely accepted ^{31}P NMR spectral assignments, and raise important questions regarding the use of TMPO and other probe molecules to study zeolite Brønsted and Lewis acid sites. We show that changes in ^{31}P NMR chemical shifts, usually attributed to differences in acid strengths, may also arise from distinct stabilization energies of $TMPOH^{+}$ ions resulting from confinement effects in ZSM-5 channels. 2D ^{1}H-^{31}P heteronuclear correlation (HETCOR) NMR experiments of HZSM-5 samples carefully loaded with varying amounts of TMPO per Al framework site, combined with DFT and AIMD calculations, provide the best description of the TMPO species formed upon interaction with zeolite acid sites.

RESULTS AND DISCUSSION

TMPO loading and NMR assessment of acid strength

Previous studies of TMPO-loaded solid acid catalysts have identified a clear separation of the ^{31}P NMR chemical shift ranges of Brønsted and Lewis acid sites interacting with TMPO, respectively, 60 - 86 ppm and 55 - 60 ppm.[1] ^{31}P NMR resonances above 86 ppm were assigned to TMPO molecules interacting with superacid sites.[13,15] Although a linear correlation between TMPO ^{31}P NMR chemical shifts and Brønsted acid site strength suggested the presence of heterogeneous acid strengths in zeolites,[20] it is widely accepted that zeolites with high Si/Al ratios, without defects such as extraframework Al species (Figure S1), contain acid sites with homogenous strength, regardless of the acid site siting and the zeolite framework type.[21,31] Although Al pairing, in the form of Al-O-Si-O-Al moieties, has been identified as the major factor influencing zeolite acid site strength,[32] ^{29}Si MAS NMR shows that such Al pairs are not present (or are too dilute to be detected) in the high Si/Al sample used, as Q^{4}(2Al) Si resonances are not observed (Figure S2).

Figure 1 shows ^{13}P MAS NMR spectra of HZSM-5 loaded with 4 mg (P/Al = 0.75), 2 mg (P/Al = 0.38) and 1 mg (P/Al = 0.21) of TMPO, corresponding to P/Al ratios of 0.75, 0.38 and 0.21, respectively. These ratios indicate that the samples (even at the highest TMPO loading) contain less than 1 TMPO molecule per framework Al site, in other words, less than one TMPO molecule per Brønsted acid site. Increasing the amount of TMPO from P/Al = 0.21 to 0.75 mg increases the ^{31}P NMR resonances at chemical shifts (δ) *ca.* 64 and 50 ppm relatively to the resonances above 69 ppm. While at the lowest TMPO-loading (P/Al = 0.21) the Brønsted acid ^{31}P NMR resonances (δ_P = 87, 84, 76 and 69 ppm) account for *ca.* 70% of the overall spectral intensity, at higher TMPO-loadings these signals comprise only 32 (P/Al = 0.38) and 23% (P/Al = 0.75), see Table S1. According to previous interpretations, increasing ^{31}P NMR chemical shifts are proportional to increasing acid strengths.[15,20] Therefore, the observed signal intensity loss in the Brønsted region (δ_P > 69 ppm), due to larger amounts of confined TMPO, would mean that the sample with the lowest TMPO content (P/Al = 0.21) should contain a larger number of strong acid sites than the samples with higher TMPO loadings. In other words, the acid strength should change with varying amounts of probe molecules.[5] However, because the P/Al = 0.21, P/Al = 0.38 and P/Al = 0.75 samples correspond to

exactly the same synthesis batch, with only different amounts of TMPO (Figure 1), it is clear that different adsorbate loadings strongly affect the spectra, and their interpretation.

It is known that TMPO excess leads to physisorbed (*ca.* 29 ppm) and crystallized (*ca.* 41 ppm) TMPO. Figure 1**Error! Reference source not found.** shows, however, that such TMPO forms remain scarce for all TMPO-loaded zeolite samples, whereas the ^{31}P NMR resonances at *ca.* 64 and 50 ppm increase at higher TMPO content. We have previously suggested the possible formation of higher-order complexes, such as $(TMPO)_2H^+$ dimers,[18] and here we shall show that these are ascribed to the 60 and 50 ppm peaks.

Although several studies report on TMPO-adsorbed zeolites, the identification of acid site siting is contentious, as most phosphorous-bearing molecules studies are based only on ^{31}P NMR chemical shift evidence. Therefore, we endeavor to revisit the assignment of the ^{31}P NMR spectra combining ^{1}H and ^{31}P chemical shift evidence and both static DFT and molecular dynamics calculations. To unambiguously assign ^{31}P resonances, we performed 2D ^{1}H-^{31}P HETCOR NMR experiments that afford additional signal discrimination, allowing to map P···H internuclear proximities between the TMPO phosphorous and the Brønsted acid sites (bridging OH group).

The most important information retrieved from ^{1}H-^{31}P HETCOR NMR is the following: ^{1}H resonances above 10 ppm are assigned to acid protons interacting with TMPO molecules, while resonances at 1-2 ppm arise from the autocorrelation between TMPO phosphorus and the methyl protons thereof.[18] The absence of the ^{1}H NMR resonance at 4.3 ppm ascribed to the unperturbed HZSM-5 Brønsted acid site,[33] indicates that these sites are engaged in H-bonds with TMPO, resulting in the considerable deshielding of this resonance to 11 - 16 ppm. The ^{1}H-^{31}P HETCOR NMR spectra of the samples P/Al = 0.38 and P/Al = 0.75 exhibit the U-shaped contour between 40 and 80 ppm observed previously,[18] witnessing the presence of multiple components at high TMPO-loadings. At low TMPO-loadings this spectral region is dominated by a single cross-peak at δ_H = 12 and δ_P = 76 ppm (Figure 2, P/Al = 0.21). While the P/Al = 0.21 ^{1}H NMR resonance at 12 ppm contains a single component, at higher TMPO-loading this region contains more than a single ^{1}H resonance, indicating the presence of distinct ^{1}H chemical environments.

Increasing the TMPO-loading up to P/Al = 0.75 (4 mg) populates the right side of the U-shaped contour, at $\delta_P \leq 60$ ppm. A projection (Figure 2, right) extracted at δ_H = 11-16 ppm shows that the ^{31}P NMR resonances at 60 - 40 ppm increase at the expenses of the *ca.* 87, 76 and 69 ppm resonances, with increasing TMPO loadings. This suggests that when the TMPO concentration inside the pores threshold is reached, high-order TMPO complexes (appearing at $\delta_P \sim 60$ and 52 ppm) form, depleting the initially formed 1:1 (TMPO:Brønsted) complexes. Although a similar behavior was reported recently by Feng Deng's group, they observed additional correlation peaks due to the use of a wet adsorption mode, arising from the interaction between TMPO and dichloromethane.[34] The presence of solvent molecules even after a high-temperature treatment indicates that a sublimation method, as reported here, is desirable to avoid

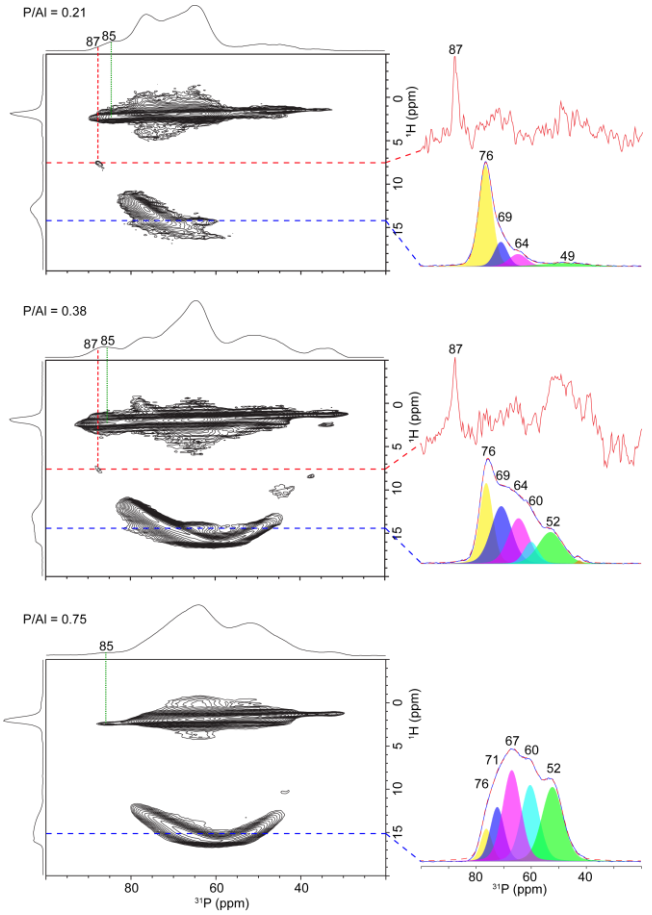

Figure 2. ^{1}H-^{31}P HETCOR NMR spectra of HZSM-5 samples loaded with 1 (P/Al = 0.21), 2 (P/Al = 0.38) and 4 mg (P/Al = 0.75) of TMPO and top projections (right side) of relevant spectral regions. The blue area depicts the region associated with 1:1 ($TMPOH^+\cdots Z^-$) and 2:1 complexes ($(TMPO)_2H^+\cdots Z^-$) and the dashed red line depicts the regions associated only with 1:1 $TMPOH^+\cdots Z^-$ complexes.

TMPO···solvent interactions, that thwart the interpretation of the ^{31}P and ^{1}H-^{31}P NMR spectra.

While most ^{31}P NMR resonances in Figure 2 correlate with ^{1}H resonances at high chemical shifts (11 - 16 ppm), the peak at *ca.* 85 ppm shows no correlation, other than the autocorrelation with the TMPO methyl protons. This behavior does not change for all TMPO-loadings suggesting that this ^{31}P NMR resonance is ascribed to a TMPO molecule interacting with a Lewis acid site (TMPO···Al), *i.e.,* not hydrogen-bonded to Brønsted acid sites. This is at odds with most studies of TMPO-loaded acid catalysts, as the 85 ppm peak is often assigned to TMPO in interaction with Brønsted superacid sites.[20] Nevertheless, previous work has also indicated that high ^{31}P NMR chemical shifts may be due to the interaction of TMPO and Lewis acid sites, thus lending support to our assignment.[16,17] On the other hand, Figure 2 shows that the ^{31}P resonance at 87 ppm correlates with the ^{1}H resonance at 7.5 ppm, indicating that it arises from a protonated TMPO. Although this phosphorous environment has been assigned as the threshold for superacidity,[20] in the following section a very distinct interpretation for this TMPO species will be given.

Locating Brønsted sites by ^{1}H-^{31}P NMR and Al/H site modeling

According to Boronat and Corma, measurements using strong bases, such as NH_3 and pyridine, can lead to the identification of an apparent heterogeneity of acid strength, arising from changes in the stabilization of the protonated base by the surrounding framework, and not changes in the intrinsic strength of the acid site.[25] We believe this statement is especially important in the context of NMR studies, as the chemical environment surrounding and stabilizing the probe molecule will strongly influence the observed chemical shifts. Note that the TMPO basicity (proton affinity (PA) of 909.7 kJ/mol) is comparable to other well-known probe molecules such as NH_3 (PA = 853.6 kJ/mol) and pyridine (PA = 930 kJ/mol), frequently used to study Bronsted acidity.[35]

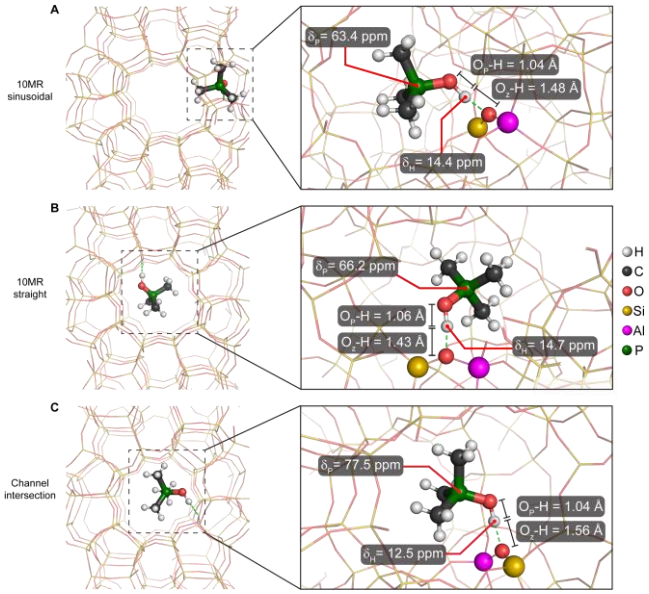

Figure 3. HZSM-5 zeolite framework viewed along the crystallographic b-axis (A, B and C). Geometry optimized TMPO:Brønsted acid 1:1 models showing the $TMPOH^+$ ion at the (A) 10MR sinusoidal channel, (B) at the 10MR straight channel, and (C) at the channel intersection. Calculated ^{1}H and ^{31}P NMR chemical shifts are depicted for each model along with the interatomic distances between the acidic proton and the zeolite oxygen (O_Z-H) and TMPO oxygen atoms (O_P-H).

As with NH_3 and Pyridine, TMPO should always form a protonated ion upon interaction with zeolite Brønsted acid sites, and is not hydrogen-bonded, as previously thought.[20] In a preceding work, we have also found that models of 1:1 and 2:1 protonated complexes may be used to fit ^{1}H and ^{31}P NMR experimental data.[18]

The MFI structure consists of two 10MR channel systems, sinusoidal and straight channels (small cavities), forming large cavities at their intersection that offer, at least, three distinct confined environments for TMPO adsorbed onto HZSM-5 acid sites. Herein, we assess the influence of TMPO confinement on the ^{1}H and ^{31}P NMR chemical shifts by studying the interaction of one TMPO molecule with Brønsted acid sites on the said three cavities. Modeling 1:1 complexes (1 TMPO per acid site) residing on these cavities was carried out by DFT (Figure S3, path 1), showing that TMPO captures the acid proton to form a $TMPOH^+\cdots Z^-$ ion pair, encompassing a protonated molecule ($TMPOH^+$) and a negatively charged zeolite framework (Z^-). Acid site siting influences the degree of proton transfer, evaluated by changes in the distance between the acid proton and both the bridging hydroxyl oxygen atom (O_Z-H) and the TMPO oxygen atom (O_P-H). At the 10MR sinusoidal (Figure 3A) and straight (Figure 3B) channels, $TMPOH^+$ ions stay closer to the negatively charged framework (O_Z-H = 1.48 and 1.43 Å, respectively) when compared with $TMPOH^+$ at the channel intersection (O_Z-H = 1.56 Å, Figure 3C). The $TMPOH^+$ ions at the 10MR sinusoidal channel and channel intersection, exhibit shorter O_P-H bond lengths, 1.04 Å, compared to $TMPOH^+$ at the 10MR straight channel, 1.06 Å (Figure 3). Previous studies have correlated the O_P-H bond length and the ^{31}P NMR chemical shifts, showing that shorter O_P-H bond lengths result in larger chemical shifts.[20,30] However, our results do not follow such trend. For example, although the O_P-H bond lengths for the three types of cavities are very similar (in two cases O_P-H bond lengths are identical – 1.04 A, Figure 3), the ^{31}P NMR chemical shifts span a large Brønsted region of ca. 15 ppm, that is, modeling $TMPOH^+$ ions in these three cavities yields calculated ^{31}P chemical shifts δ_P = 77.5 ppm (Figure 3C), δ_P = 66.2 ppm (Figure 3B), and δ_P = 63.4 ppm (Figure 3A). These values are in good agreement with the experimentally observed *ca.* 77, 69 and 64 ppm, respectively. A similar agreement is found for calculated and experimental ^{1}H chemical shifts. Table S2 compiles experimental and calculated chemical shifts of TMPO molecules adsorbed on the distinct cavities.

Hernandez-Tamargo *et al.,* suggested that upon TMPO protonation the $TMPOH^+$ ion can move away from the original Brønsted site to a pure silica channel intersection, and that this ion could be the origin of the highly deshielded peak at δ_P > 86 ppm.[30] However, neither the ^{1}H nor the ^{31}P NMR chemical shifts were calculated for this species. To test this hypothesis, we have generated a model in which a $TMPOH^+$ ion at the channel intersection interacting with an acid site (Figure 3C), is displaced towards the closest channel intersection with no acid site, *i.e.*, a pure silica channel intersection (Figure 4). This step was followed by DFT geometry optimization of the $TMPOH^+$ / pure-silica channel intersection system, which led to the shortening of the O_P-H bond length, from 1.04 to 0.99 Å (Figure 3C and Figure 4). The calculated ^{1}H and ^{31}P NMR chemical shifts were δ_P = 85.9 and δ_H = 8.07 ppm. These results corroborate the

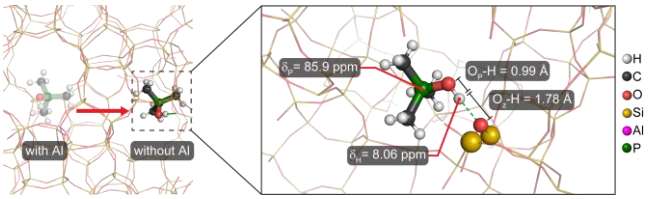

Figure 4. HZSM-5 zeolite framework viewed along the crystallographic a-axis, showing the displacement (left) of the $TMPOH^+$ from the channel intersection close to a Brønsted acid site (Figure 3C) to a pure-silica channel intersection, prior to geometry optimization of the $TMPOH^+$ ion interacting with a Si-O-Si moiety. Calculated ^{1}H and ^{31}P NMR chemical shifts are depicted along with the interatomic distances between the acidic proton and the zeolite oxygen (O_Z-H) and TMPO oxygen (O_P-H) atoms.

assignment of the cross peak at δ_P = 87 ppm; δ_H = 7.5 (Figure 2) to $TMPOH^+$ ions hydrogen-bonded to a Si-O-Si moiety at the zeolite channel intersection with no framework Al sites.

To summarize, DFT shows that the experimental ^{31}P NMR chemical shifts at 64, 69 and 76 ppm arise from $TMPOH^+$ ions located in the: 10MR sinusoidal channel (Figure 3A), 10MR straight channel (Figure 3B), and channel intersection close to a Brønsted acid site (Figure 3C), respectively. The ^{31}P NMR chemical shift at 87 ppm is ascribed to $TMPOH^+$ ions at the pure silica channel intersection (Figure 4). The differences in ^{31}P chemical shift expose the distinct confinement of $TMPOH^+$ ions residing in different cavities, rather than revealing differences in Brønsted acid strengths.

TMPO dimerization, $(TMPO)_2H^+$

Al-containing and siliceous channel intersections

Using MC methods, a second TMPO molecule was placed close to a $TMPOH^+$ ion interacting with the Brønsted acid site at the channel intersection (Figure 3C), followed by DFT structure relaxation (Figure S3, Path 4). The outcome of these calculations consists of two non-interacting TMPO and $TMPOH^+$ molecules giving peaks at δ_P = 75.8 and 22.4 ppm, respectively (Figure S4A and B). In contrast, if the second TMPO molecule is close to $TMPOH^+$ at the pure-silica channel intersection a $(TMPO)_2H^+$ dimer forms instead with δ_P = 60.3 and 37.3 ppm (Figure S4C and D). In both cases, the calculated ^{31}P NMR chemical shifts are outside the experimental range (δ_P = 40 to 87 ppm). These findings show that conventional DFT-based geometry optimization of $(TMPO)_2H^+$ species is of limited use in spectral assignment. A better correlation between theoretical and experimental data was obtained after performing a 2.5 ps AIMD calculation at 423 K (temperature of HSZM-5 TMPO adsorption) using the same starting point of the DFT-based calculation (Figure S3, Path 6). Increasing the temperature had a strong impact on TMPO speciation, favoring the formation of a $(TMPO)_2H^+$ ion in both channel intersections above-mentioned. The trajectories of these AIMD calculations (Video S1 and S2) show the TMPO molecule approaching the $TMPOH^+$ ion to form a hydrogen bonded $(TMPO)_2H^+$ dimer, which moves away from the zeolite framework to the center of the channel intersection, as evidenced by the elongation of the O_Z-H bond (Table S3). Although the formation of a $TMPOH^+$ ion sharing with a free TMPO molecule the same cavity (Figure S4A and B) is energetically more favorable than the formation of $(TMPO)_2H^+$ dimers (Figure 5A), only the calculated ^1H and ^{31}P chemical shifts of the latter (δ_H = 15.4 ppm; δ_{P1} = 51.2 and δ_{P2} = 45.2 ppm) are in accord with the experimental data. Moreover, when two TMPO molecules share a pure silica channel intersection the $(TMPO)_2H^+$ dimer also forms (Figure 5B), albeit in the absence of the Brønsted acid site, giving calculated chemical shifts δ_H = 16.9 ppm, δ_{P1} = 57.7 and δ_{P2} = 53.4 ppm (Table S4). These values are in fair agreement with the experimental ^{31}P NMR resonances at 60 and 52 ppm observed at higher TMPO-loadings (Figure 2), in contrast, with the $(TMPO)_2H^+$ dimer formed in the same location using DFT-based calculations (Figure S4C and D, Table S4). These dimer peaks increase as the δ_P = 87 and 76 ppm $TMPOH^+$ resonances decrease. This strongly supports the conversion of 1:1 complexes residing in these cavities into $(TMPO)_2H^+$ dimers, showing that the AIMD step is essential to model the higher-order complexes formed upon high temperature (423 K) TMPO adsorption on zeolites. However, modeling 1:1 TMPO-Brønsted acid complexes with AIMD calculations, followed by a DFT optimisation (see flow chart Figure S7), afforded ^1H and ^{31}P NMR chemical shifts comparable to DFT calculations at 0 K (Table S5-S8), without prior AIMD.

^{31}P double quantum-filtering (DQF) NMR experiments of the P/Al = 0.21 (1 mg TMPO) and 1.3 (6 mg TMPO) samples are shown in Figure S7. No signal is observed for the lowest TMPO loading after more than 40 hours of acquisition. This is attributed to many factors, including the very small TMPO amounts, the low excitation efficiency of DQF experiments and the low amount of $(TMPO)_2H^+$ dimers. At the highest TMPO-loading, the ^{31}P DQF spectrum exhibits a resonance typical of both 1:1 and 2:1 complexes. The ^{31}P resonances above 60 ppm, assigned to 1:1 complexes, arise from P-P proximities involving two neighbor 1:1 complexes and/or between 1:1 and 2:1 complexes. In fact, due to the small distance between the center of the 10MR channels and the channel intersection (~4 Å), TMPO molecules residing in distinct cavities may also contribute to the DQ signal, hence precluding the unambiguous identification of the distinct TMPO complexes.

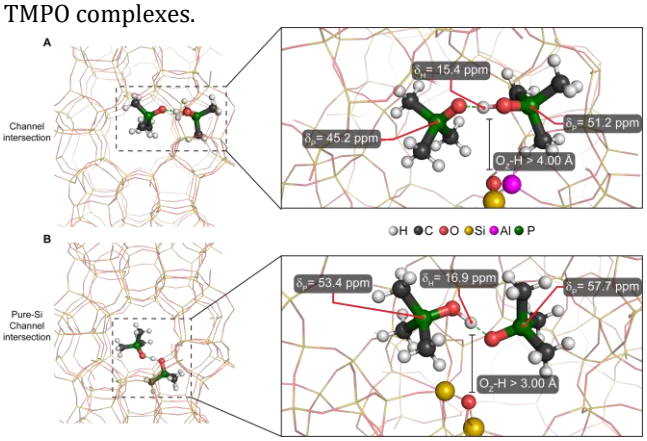

Figure 5. HZSM-5 zeolite framework viewed along the crystallographic b-axis (A, B). TMPO:Brønsted acid 2:1 models, optimized using AIMD followed by DFT geometry optimization, showing the $(TMPO)_2H^+$ dimer A) at the channel intersection and B) at pure-silica channel intersection, i.e., with no framework Al sites. Calculated ^1H and ^{31}P NMR chemical shifts are depicted for each model along with the interatomic distances between the acidic proton and and the zeolite oxygen (O_Z-H) and TMPO oxygen atoms (O_P-H).

10MR channels

Adding a second TMPO molecule to the $TMPOH^+$ ion at the 10MR straight channels does not result in the formation of $(TMPO)_2H^+$ dimers (Figure S5). Instead, a $TMPOH^+$ ion and a free TMPO molecule at distinct channel intersections (Figure S5C and D) form. Thus, when two TMPO molecules meet in the 10MR straight channels the AIMD trajectories favor their separation, placing them at different channel intersections along the 10MR longitudinal axis. Moreover, the calculated ^1H and ^{31}P NMR chemical shifts of these TMPO species are not in accord with the experimental data (Table S9).

Although DFT and AIMD-based calculations indicate that TMPO dimerizes at the 10MR sinusoidal channels (Figure S6 and Table S10), ^{1}H and ^{31}P calculated NMR chemical shifts are at odds with the experimental evidence. Note that the $(TMPO)_2H^+$ dimer forms between the sinusoidal channel and the channel intersection, not in the 10MR sinusoidal channel (Figure S6). In practice, we have a higher amount of TMPO molecules per unit cell as compared to theoretical calculations, which may hinder TMPO dynamics inside the zeolite cavities, thus increasing the likelihood of TMPO dimerization, even in the 10MR channels.

CONCLUSIONS

While TMPO has been widely used as a probe molecule in NMR studies of zeolite catalysts, the assignment of ^{31}P NMR resonances remains a matter of considerable debate. The present work shows that ^{1}H-^{31}P HETCOR NMR combined with both a careful TMPO zeolite loading and molecular modeling provide new insight into the nature of the TMPO···HZSM-5 interactions. At low TMPO-loading, the formation of 1:1 complexes (one TMPO per Brønsted acid site) is favored, resulting in ^{31}P NMR resonances at *ca*. 87, 76, 69 and 64 ppm. DFT-based geometry optimization of such complexes indicates that these resonances arise from the different siting of the protonated TMPO in the HZSM-5 pores (confinement effect), namely at the 10MR sinusoidal (δ_P = 64 ppm) and straight channels (δ_P = 69 ppm), and at the channel intersections in the presence (δ_P = 76 ppm) or absence (δ_P = 87 ppm) of a nearby Brønsted acid site. Thus, these ^{31}P NMR resonances are not given by TMPO molecules interacting with sites of different Brønsted acid strengths, corroborating the current tenet that zeolite Brønsted acid strength is homogeneous (Figure 2, P/Al = 0.21).

AIMD-based calculations considering the experimental temperature, 423 K, provide insight into the nature of TMPO interaction with the HZSM-5 framework and with a second TMPO molecule, showing that even at low loadings, some molecules form $(TMPO)_2H^+$ dimers (^{31}P resonances in the 40 to 60 ppm range). It is worth noting that DFT optimizations, which can find only the nearest local minimum when starting from a given configuration, were unable to provide evidence for the presence of such dimers. Although DFT could be used to model 1:1 TMPO-Brønsted acid complexes, modeling both 1:1 and 2:1 TMPO-Brønsted acid complexes was only possible using AIMD calculations followed by DFT optimisations to bring the structure to the nearest local minimum.

However, modeling 1:1 TMPO-Brønsted acid complexes with AIMD calculations afforded ^{1}H and ^{31}P NMR chemical shifts comparable to DFT calculations at 0 K (Table S5-S8).

We believe that high-order complexes are likely to form in other probe molecules with similar base strengths, such as NH_3 and pyridine. Strong bases can easily remove the proton from zeolite Brønsted acid sites, forming their respective conjugate acid, that may in turn interact with neighbor 'non-protonated' probe molecules to generate dimers and possibly trimers. While the formation of dimers has been reported for NH_3,[36,37] pyridine [38,39] and TMPO,[18,40] most studies ignore the formation thereof. The formation of high-order complexes deserves further investigation, as many probe molecules are now used routinely to study the acidity of several solid-acid catalysts. Importantly, the quantification of Brønsted acid sites using adsorbed probe molecules may indeed be compromised if the formation of high-order complexes is not considered. The degree of probe molecule dimerization will inevitably change the Brønsted:(probe molecule) stoichiometry, thus contributing to the overestimation in the amount of acid sites.

In summary, the use of P-bearing probe molecules to assess by NMR zeolite Brønsted acidity has many limitations and is prone to erroneous conclusions. This is likely to be the case for other probe molecules exhibiting strong basicity.

ASSOCIATED CONTENT

Experimental procedures, ^{27}Al and ^{29}Si solid-state NMR spectra of HZSM-5 sample, supplementary data about DFT, AIMD and AIMD+DFT calculations of 1:1 and 2:1 complexes and calculated ^{31}P and ^{1}H chemical shifts (PDF). AIMD trajectories of the formation of 2:1 complexes are provided in AVI format (ZIP). The Supporting Information is available free of charge at http://pubs.acs.org.

AUTHOR INFORMATION

Corresponding Author

* lmafra@ua.pt

Author Contributions

The manuscript was written through contributions of all authors.

Notes

The authors declare no competing financial interest.

ACKNOWLEDGMENT

C. Bornes acknowledges FCT for the doctoral fellowship PD/BD/142849/2018 integrated in the PhD Program in NMR applied to chemistry, materials and biosciences (PD/00065/2013). This work was developed within the scope of the project CICECO-Aveiro Institute of Materials, UIDB/50011/2020 & UIDP/50011/2020, financed by national funds through the FCT/MEC and when appropriate cofinanced by FEDER under the PT2020 Partnership Agreement. We also thank FCT for funding the project PTDC/QEQ-QAN/6373/2014. The NMR spectrometers are part of the National NMR Network (PTNMR) and are partially supported by Infrastructure Project No. 022161 (co-financed by FEDER through COMPETE 2020, POCI and PORL and FCT through PIDDAC). This work has received funding from the European Research Council (ERC) under the European Union's Horizon 2020 research and innovation program (grant agreement no. 865974). M. Fischer acknowledges funding by the Deutsche Forschungsgemeinschaft (DFG; German Research Foundation), project number 389577027 (FI1800/5-1). This work was supported by the North-German Supercomputing Alliance (HLRN).

ABBREVIATIONS

TMPO, trimethylphosphine oxide; NMR, nuclear magnetic resonance; DFT, density functional theory; AIMD, ab initio molecular dynamics.

REFERENCES

(1) Vimont, A.; Daturi, M.; Winfield, J. M. Investigation of Surface Acidity Using a Range of Probe Molecules. In *Functionalized Inorganic Fluorides*; Tressaud, A., Ed.; John Wiley & Sons, Ltd: Chichester, UK, 2010; pp 101–139.

(2) Yi, X.; Xiao, Y.; Li, G.; Liu, Z.; Chen, W.; Liu, S.-B.; Zheng, A. From One to Two: Acidic Proton Spatial Networks in Porous Zeolite Materials. *Chemistry of Materials* **2020**, *32* (3), 1332–1342. https://doi.org/10.1021/acs.chemmater.0c00005.

(3) Romero; Marie, O.; Saussey, J.; Daturi, M. Infrared Evidence of Three Distinct Acidic Hydroxyls in Defect-Free HY Faujasite. *J. Phys. Chem. B* **2005**, *109* (5), 1660–1662. https://doi.org/10.1021/jp045333n.

(4) Rakiewicz, E. F.; Peters, A. W.; Wormsbecher, R. F.; Sutovich, K. J.; Mueller, K. T. Characterization of Acid Sites in Zeolitic and Other Inorganic Systems Using Solid-State 31 P NMR of the Probe Molecule Trimethylphosphine Oxide. *J. Phys. Chem. B* **1998**, *102* (98), 2890–2896. https://doi.org/10.1021/jp980808u.

(5) Yi, X.; Zheng, A.; Liu, S.-B. Acidity Characterization of Solid Acid Catalysts by Solid-State ^{31}P NMR of Adsorbed Phosphorus Containing Probe Molecules: An Update. In Annual Reports on NMR Spectroscopy; Atta-ur-Rahman, Ed.; Academic Press, 2020, Vol. 101, 65–149.

(6) Hayashi, S.; Kojima, N. Acid Properties of H-Type Mordenite Studied by Solid-State NMR. *Microporous and Mesoporous Materials* **2011**, *141* (1–3), 49–55. https://doi.org/10.1016/j.micromeso.2009.11.006.

(7) Hayashi, S.; Jimura, K.; Kojima, N. Adsorption of Trimethylphosphine Oxide on Silicalite Studied by Solid-State NMR. *Bulletin of the Chemical Society of Japan* **2014**, *87* (1), 69–75. https://doi.org/10.1246/bcsj.20130192.

(8) Zhao, R.; Zhao, Z.; Li, S.; Zhang, W. Insights into the Correlation of Aluminum Distribution and Brönsted Acidity in H-Beta Zeolites from Solid-State NMR Spectroscopy and DFT Calculations. *Journal of Physical Chemistry Letters* **2017**, *8* (10), 2323–2327. https://doi.org/10.1021/acs.jpclett.7b00711.

(9) Trickett, C. A.; Osborn Popp, T. M.; Su, J.; Yan, C.; Weisberg, J.; Huq, A.; Urban, P.; Jiang, J.; Kalmutzki, M. J.; Liu, Q.; Baek, J.; Head-Gordon, M. P.; Somorjai, G. A.; Reimer, J. A.; Yaghi, O. M. Identification of the Strong Brønsted Acid Site in a Metal–Organic Framework Solid Acid Catalyst. *Nature Chem* **2019**, *11* (2), 170–176. https://doi.org/10.1038/s41557-018-0171-z.

(10) Jiang, J.; Gándara, F.; Zhang, Y.-B.; Na, K.; Yaghi, O. M.; Klemperer, W. G. Superacidity in Sulfated Metal–Organic Framework-808. *J. Am. Chem. Soc.* **2014**, *136* (37), 12844–12847. https://doi.org/10.1021/ja507119n.

(11) Huang, S. J.; Yang, C. Y.; Zheng, A.; Feng, N.; Yu, N.; Wu, P. H.; Chang, Y. C.; Lin, Y. C.; Deng, F.; Liu, S. B. New Insights into Keggin-Type 12-Tungstophosphoric Acid from ^{31}P MAS NMR Analysis of Absorbed Trimethylphosphine Oxide and DFT Calculations. *Chemistry - An Asian Journal* **2011**, *6* (1), 137–148. https://doi.org/10.1002/asia.201000572.

(12) Yang, J.; Janik, M. J.; Ma, D.; Zheng, A.; Zhang, M.; Neurock, M.; Davis, R. J.; Ye, C.; Deng, F. Location, Acid Strength, and Mobility of the Acidic Protons in Keggin 12-H3PW12O40: A Combined Solid-State NMR Spectroscopy and DFT Quantum Chemical Calculation Study. *Journal of the American Chemical Society* **2005**, *127* (51), 18274–18280. https://doi.org/10.1021/ja055925z.

(13) Zheng, A.; Huang, S. J.; Chen, W. H.; Wu, P. H.; Zhang, H.; Lee, H. K.; De Ménorval, L. C.; Deng, F.; Liu, S. B. ^{31}P Chemical Shift of Adsorbed Trialkylphosphine Oxides for Acidity Characterization of Solid Acids Catalysts. *Journal of Physical Chemistry A* **2008**, *112* (32), 7349–7356. https://doi.org/10.1021/jp8027319.

(14) Lang, S.; Benz, M.; Obenaus, U.; Himmelmann, R.; Hunger, M. Novel Approach for the Characterization of Lewis Acidic Solid Catalysts by Solid-State NMR Spectroscopy. *ChemCatChem* **2016**, *8* (12), 2031–2036. https://doi.org/10.1002/cctc.201600372.

(15) Zheng, A.; Liu, S. B.; Deng, F. ^{31}P NMR Chemical Shifts of Phosphorus Probes as Reliable and Practical Acidity Scales for Solid and Liquid Catalysts. *Chemical Reviews* **2017**, *117* (19), 12475–12531. https://doi.org/10.1021/acs.chemrev.7b00289.

(16) Wiper, P. V.; Amelse, J.; Mafra, L. Multinuclear Solid-State NMR Characterization of the Brønsted/Lewis Acid Properties in the BP HAMS-1B (H-[B]-ZSM-5) Borosilicate Molecular Sieve Using Adsorbed TMPO and TBPO Probe Molecules. *Journal of Catalysis* **2014**, *316*, 240–250. https://doi.org/10.1016/j.jcat.2014.05.017.

(17) Chen, W. H.; Ko, H. H.; Sakthivel, A.; Huang, S. J.; Liu, S. H.; Lo, A. Y.; Tsai, T. C.; Liu, S. B. A Solid-State NMR, FT-IR and TPD Study on Acid Properties of Sulfated and Metal-Promoted Zirconia: Influence of Promoter and Sulfation Treatment. *Catalysis Today* **2006**, *116* (2 SPEC. ISS.), 111–120. https://doi.org/10.1016/j.cattod.2006.01.025.

(18) Bornes, C.; Sardo, M.; Lin, Z.; Amelse, J.; Fernandes, A.; Ribeiro, M. F.; Geraldes, C.; Rocha, J.; Mafra, L. ^{1}H-^{31}P HETCOR NMR Elucidates the Nature of Acid Sites in Zeolite HZSM-5 Probed with Trimethylphosphine Oxide. *Chemical Communications* **2019**, *55* (84), 12635–12638. https://doi.org/10.1039/c9cc06763a.

(19) Pires, E.; Fraile, J. M. Study of Interactions between Brønsted Acids and Triethylphosphine Oxide in Solution by ^{31} P NMR: Evidence for 2 : 1 Species. *Phys. Chem. Chem. Phys.* **2020**, *22* (42), 24351–24358. https://doi.org/10.1039/D0CP03812A.

(20) Zheng, A.; Zhang, H.; Lu, X.; Liu, S. B.; Deng, F. Theoretical Predictions Of ^{31}P NMR Chemical Shift Threshold of Trimethylphosphine Oxide Absorbed on Solid Acid Catalysts. *Journal of Physical Chemistry B* **2008**, *112* (15), 4496–4505. https://doi.org/10.1021/jp709739v.

(21) Jones, A. J.; Iglesia, E. The Strength of Brønsted Acid Sites in Microporous Aluminosilicates. *ACS Catalysis* **2015**, *5* (10), 5741–5755. https://doi.org/10.1021/acscatal.5b01133.

(22) Brändle, M.; Sauer, J. Acidity Differences between Inorganic Solids Induced by Their Framework Structure. A Combined Quantum Mechanics/Molecular Mechanics Ab Initio Study on Zeolites. *J. Am. Chem. Soc.* **1998**, *120* (7), 1556–1570. https://doi.org/10.1021/ja9729037.

(23) Jones, A. J.; Carr, R. T.; Zones, S. I.; Iglesia, E. Acid Strength and Solvation in Catalysis by MFI Zeolites and Effects of the Identity, Concentration and Location of Framework Heteroatoms. *Journal of Catalysis* **2014**, *312*, 58–68. https://doi.org/10.1016/j.jcat.2014.01.007.

(24) Sauer, J.; Sierka, M. Combining Quantum Mechanics and Interatomic Potential Functions in Ab Initio Studies of Extended Systems. *Journal of Computational Chemistry* **2000**, *21* (16), 1470–1493. https://doi.org/10.1002/1096-987X(200012)21:16<1470::AID-JCC5>3.0.CO;2-L.

(25) Boronat, M.; Corma, A. What Is Measured When Measuring Acidity in Zeolites with Probe Molecules? *ACS Catalysis* **2019**, *9* (2), 1539–1548. https://doi.org/10.1021/acscatal.8b04317.

(26) Góra-Marek, K.; Melián-Cabrera, I. A Note on the Acid Strength of Porous Materials Assessed by Thermal Methods. *Microporous and Mesoporous Materials* **2021**, *310*, 110638. https://doi.org/10.1016/j.micromeso.2020.110638.

(27) Bailleul, S.; Yarulina, I.; Hoffman, A. E. J.; Dokania, A.; Abou-Hamad, E.; Chowdhury, A. D.; Pieters, G.; Hajek, J.; De Wispelaere, K.; Waroquier, M.; Gascon, J.; Van Speybroeck, V. A Supramolecular View on the Cooperative Role of Brønsted and Lewis Acid Sites in Zeolites for Methanol Conversion. *Journal of the American Chemical Society* **2019**, *141* (37), 14823–14842. https://doi.org/10.1021/jacs.9b07484.

(28) Nastase, S. A. F.; Cnudde, P.; Vanduyfhuys, L.; De Wispelaere, K.; Van Speybroeck, V.; Catlow, C. R. A.; Logsdail, A. J.

Mechanistic Insight into the Framework Methylation of H-ZSM-5 for Varying Methanol Loadings and Si/Al Ratios Using First-Principles Molecular Dynamics Simulations. *ACS Catal.* **2020**, *10* (15), 8904–8915. https://doi.org/10.1021/acscatal.0c01454.

(29) Gould, N. S.; Li, S.; Cho, H. J.; Landfield, H.; Caratzoulas, S.; Vlachos, D.; Bai, P.; Xu, B. Understanding Solvent Effects on Adsorption and Protonation in Porous Catalysts. *Nat Commun* **2020**, *11* (1), 1060. https://doi.org/10.1038/s41467-020-14860-6.

(30) Hernandez-Tamargo, C. E.; Roldan, A.; De Leeuw, N. H. DFT Modeling of the Adsorption of Trimethylphosphine Oxide at the Internal and External Surfaces of Zeolite MFI. *Journal of Physical Chemistry C* **2016**, *120* (34), 19097–19106. https://doi.org/10.1021/acs.jpcc.6b03448.

(31) Deshlahra, P.; Iglesia, E. Reactivity Descriptors in Acid Catalysis: Acid Strength, Proton Affinity and Host–Guest Interactions. *Chem. Commun.* **2020**, *56* (54), 7371–7398. https://doi.org/10.1039/D0CC02593C.

(32) Grajciar, L.; Areán, C. O.; Pulido, A.; Nachtigall, P. Periodic DFT Investigation of the Effect of Aluminium Content on the Properties of the Acid Zeolite H-FER. *Phys. Chem. Chem. Phys.* **2010**, *12* (7), 1497. https://doi.org/10.1039/b917969k.

(33) Hunger, M. Multinuclear Solid-State NMR Studies of Acidic and Non-Acidic Hydroxyl Protons in Zeolites. *Solid State Nuclear Magnetic Resonance* **1996**, *6* (1), 1–29. https://doi.org/10.1016/0926-2040(95)01201-X.

(34) Wang, Y.; Xin, S.; Chu, Y.; Xu, J.; Qi, G.; Wang, Q.; Xia, Q.; Deng, F. Influence of Trimethylphosphine Oxide Loading on the Measurement of Zeolite Acidity by Solid-State NMR Spectroscopy. *J. Phys. Chem. C* **2021**, *125* (17), 9497–9506. https://doi.org/10.1021/acs.jpcc.1c01789.

(35) National Institute of Standards and Technology. NIST Web-Book https://webbook.nist.gov/chemistry/ (accessed 2021 -04 -22).

(36) Barthos, R.; Lónyi, F.; Onyestyák, Gy.; Valyon, J. An IR, FR, and TPD Study on the Acidity of H-ZSM-5, Sulfated Zirconia, and Sulfated Zirconia−Titania Using Ammonia as the Probe Molecule. *J. Phys. Chem. B* **2000**, *104* (31), 7311–7319. https://doi.org/10.1021/jp000937m.

(37) Lónyi, F.; Valyon, J. On the Interpretation of the NH3-TPD Patterns of H-ZSM-5 and H-Mordenite. *Microporous and Mesoporous Materials* **2001**, *47* (2–3), 293–301. https://doi.org/10.1016/S1387-1811(01)00389-4.

(38) Jin, F.; Li, Y. A FTIR and TPD Examination of the Distributive Properties of Acid Sites on ZSM-5 Zeolite with Pyridine as a Probe Molecule. *Catalysis Today* **2009**, *145* (1–2), 101–107. https://doi.org/10.1016/j.cattod.2008.06.007.

(39) Buzzoni, R.; Bordiga, S.; Ricchiardi, G.; Lamberti, C.; Zecchina, A.; Bellussi, G. Interaction of Pyridine with Acidic (H-ZSM5, H-β, H-MORD Zeolites) and Superacidic (H-Nafion Membrane) Systems: An IR Investigation. *Langmuir* **1996**, *12* (4), 930–940. https://doi.org/10.1021/la950571i.

(40) Feng, N.; Zheng, A.; Huang, S. J.; Zhang, H.; Yu, N.; Yang, C. Y.; Liu, S. B.; Deng, F. Combined Solid-State NMR and Theoretical Calculation Studies of Brønsted Acid Properties in Anhydrous 12-Molybdophosphoric Acid. *Journal of Physical Chemistry C* **2010**, *114* (36), 15464–15472. https://doi.org/10.1021/jp105683y.